Hydrol. Earth Syst. Sci. Discuss., 10, 325–373, 2013
www.hydrol-earth-syst-sci-discuss.net/10/325/2013/
doi:10.5194/hessd-10-325-2013

Hydrology and Earth System Sciences Discussions

Sedimentation monitoring including uncertainty analysis in complex floodplains: a case study in the Mekong Delta

N. V. Manh, B. Merz, and H. Apel

GFZ – German Research Center for Geoscience, Section 5.4 Hydrology, Potsdam, Germany

Received: 11 December 2012 – Accepted: 17 December 2012 – Published: 11 January 2013

Correspondence to: N. V. Manh (manh@gfz-potsdam.de)

Published by Copernicus Publications on behalf of the European Geosciences Union.

Abstract

Quantity and quality of sediment deposition in complex floodplains are affected by many uncertain factors, ranging from suspended sediment transport dynamics in rivers and floodplain channel interactions to internal floodplain processes. In consequence, any point measurement of sedimentation in floodplains contains a high degree of uncertainty calling for a careful analysis of the measured data. However, uncertainty analyses are not documented in publications on floodplain sedimentation data. Therefore the presented work illustrates a field sampling strategy aiming at the quantification of uncertainties associated to sediment deposition data, as well as the spatial variability of sediments deposition on floodplains. The study was performed in the Mekong Delta (MD), being an example for a large and complex floodplain with a high degree of anthropogenic disturbances. We present a procedure for the quantification of the uncertainty associated to the data, based on the design of the monitoring campaign and floodplain characteristics. Sediment traps were distributed strategically over the floodplain in clusters of three mat traps representing one monitoring point. The uncertainty originating from collection of the traps in ponding water is quantified by lab experiments. The uncertainty of a single monitoring point is then quantified in a Monte Carlo simulation, propagating the uncertainty from the different uncertainty sources to final uncertainty bounds of the monitored sediment data. For the case study area, it is shown that there are no correlations in the spatial distribution of sedimentation in floodplains. This can be explained by the highly complex channel and dike system and the high number of hydraulic structures. However, it can be shown that within single floodplain compartments the spatial deposition variability depends on the dike levels and operation and location of hydraulic structures.

HESSD
10, 325–373, 2013

1 Introduction

Sediment deposition in floodplains in river deltas is controlled by sediment delivery from the upstream catchment, but also by characteristics of the particular delta. The delivery from the catchment, i.e. the suspended sediment transport, is controlled by climate, geography, soil types, land cover, and increasingly by reservoir operation. Floodplain sedimentation in deltas can be very complex, as the spatial variability of floodplain sedimentation is frequently very high, due to natural variability and a high level of anthropogenic interference. In the Vietnamese part of the Mekong Delta (MD) this interference is extraordinarily high, as almost the complete Delta is used for agricultural production and dissected by a dense channel networks. In addition to the channels, the floodplains are compartmented by dike rings, and in case of high level dike rings the floodplain inundation is often influenced by operation of sluice gates and pumps (Hung et al., 2012). This interplay of different controlling factors suggests a high spatial variability of floodplain sedimentation (Hung et al., 2013b). However, a quantification of this variability on the large scale by measurement campaigns does not exist.

This expected spatial variability constricts the value of single point measurements. Considering also the known errors in sediment deposition measurements, it becomes clear that (a) a representative monitoring of floodplain sedimentation for a large delta is a difficult task in general, and (b) there is a clear need for a thorough estimation of the uncertainties of sedimentation data. The latter aspect facilitates a proper use and interpretation of the data and improves the credibility of the derived results and recommendations. The uncertainty analysis should identify the possible epistemic and aleatory uncertainty sources and try to quantify them.

There are a number of studies that monitor sedimentation on floodplains, often using mat traps to quantify the accumulative sediment deposition during flood events (Asselmann and Middelkoop, 1995; Steiger et al., 2001, 2003; Middelkoop et al., 2005; Büttner et al., 2006). However, none of the studies quantified the uncertainties, neither epistemic sampling uncertainty, nor aleatory uncertainty related to spatial variability.

HESSD
10, 325–373, 2013

There are publications on uncertainty analysis in sediment research (Salas and Shin, 1999; Navratil et al., 2011; Shamsudin et al., 2012). However, these studies focus on other aspects such as reservoir sedimentation, urban retention pond or suspended sediment mobilization and transport in small mountainous catchments.

This study presents a monitoring scheme aiming at the quantification of spatial variability of sediment and nutrient floodplain deposition in the MD, as well as a strategy to quantify the uncertainty of the sediment sampling scheme. The study is the first large scale monitoring of floodplain sedimentation in the MD. In addition, it also provides uncertainty estimates for the monitoring results for the first time, thus indicating the trustworthiness of sediment trap data. The data can contribute to the debate on the economic value of floodplain deposition in terms of nutrients, which is a hot topic in the MD. There is a trend to totally blocking floodplain inundation in favor of three cropping periods per year, that have to be sustained by increasing input of mineral fertilizers.

2 Study area and site selection

The Mekong Delta begins near Phnom Penh where the largest tributary, the Bassac River, branches away from the Mekong River and terminates as a huge fertile flat plain in southern Vietnam. It is known as the most complex channel network in the world and it is the habitat of more than 10 million people. The annual inundated floodplain area in the Mekong Delta in the Vietnamese territory is around 19.500 km^2 (Hung et al., 2012) with 91.061 km length of channel networks (MARD report 2011), (Fig. 1).

Deposited sediment play a very important role in agricultural development in the MD. The annual suspended sediment load into the MD at Kratie is about 160 million tons (Walling, 2008) and 110/150 million tons of total suspended solid, 60 million tons of total dissolved solid (Milliman, 2011). Approximately 80 % of Mekong delivered sediment is trapped within the delta area (Xue et al., 2010). The annual loads of total nitrogen (TN) and total phosphorous (TP) at the river mouths of the MD were estimated to be $2.7 \times 10^4\,t\,N\,a^{-1}$ and $9 \times 10^3\,t\,P\,a^{-1}$ (1987–1999) (Yoshimura et al., 2009). The annual

HESSD
10, 325–373, 2013

flood lasts from July or August to the end of November or mid-December. The main inundated areas are located in the northern part of the MD, which are differentiated into the Plan of Reeds east of the Mekong (Tien in Vietnamese) branch, the Long Xuyen Quadrangle west of the Bassac (Hau in Vietnamese) branch, and the area between the Tien and Hau rivers. A number of secondary channels connected to either the Tien or Hau River facilitate widespread distribution of the flood water to the floodplains.

The agricultural system is adapted to the annual floods. Traditionally two crops are grown around the flood period utilizing the sediments and flood waters for irrigation and as nutrient source. Recently, a third crop was introduced in the shallow inundated areas of the delta, where the flood protection systems are well developed and floodplain inundation can be controlled completely under normal flood conditions. The spatial extent of the three crop system depends on the flood magnitude and economic factors.

The study area is the entire regularly inundated floodplain in the Vietnamese part of the MD (VMD). The inundated floodplains vary year by year depending on the flood magnitude and the seasonal cropping pattern in the floodplains. These are controlled by the hydraulic structures, based communal agreements. The main difference of flood characteristics in MD to other parts of the world is that the flood event is always longer than 3 months, setting it apart not only in the spatial, but also the temporal inundation extent compared to typical inundation durations from a few days to two weeks in smaller basins. Normally, the inundation duration extends from 4 to 5 months with single or double peak hydrographs. The sedimentation rate in floodplains depends on the following factors:

1. flood magnitude (peak discharge and flood volume) and associated suspended sediment transport,
2. distance to the main channels,
3. local hydraulic regime in floodplains,
4. dike levels and operation of the hydraulic structures, and

5. other human activities in floodplains, such as fishing.

The floodplains in the VMD are intensively used, even during floods. Typically a portion of the flood water is retained in the floodplain compartments and used for paddy cultivation. Depending on the flood magnitude and duration and the dike elevations, the farmers start to pump the water from the floodplains at some point in December in order to enable growing of two crops between flood seasons (Hung et al., 2012). In most cases paddy rice is grown after the flood period, thus the farmers retain ponding water on the floodplains in the range of 20–40 cm. This has consequences for the sediment monitoring. First of all, the time for trap deployment and collection is limited, as there are just a few days between the crops and the inundation where the land is not used. The traps have to be placed in these short time windows, otherwise either the farmers will remove the traps or the positioning is not possible because the floodplains are already inundated. Besides this logistical obstacle, there is also the problem that the traps have to be collected with water still ponding on the fields. This obviously introduces measurement errors, which need to be taken into account.

During the inundation the floodplains are used for fishing, which is traditionally done with nets. This disturbs the deposition and erosion processes, but also puts the traps at risk of being destroyed. This adds additional uncertainty to the monitored sediment deposition, both by loss of traps as well as by re-suspension and relocation processes. Thus the sediment trapping and uncertainty analysis require appropriate trap design, trap installation, trap collection, and methods to quantify the uncertainties stemming from these processes.

The selected sampling sites must be representative for the different inundation regions, inundation depths and flood protection levels. The criteria for site selections sorted by descending priority are as follows:

1. The selected sites have to be distributed the main floodplains in the MD, including the Plan of Reeds, Long Xuyen quadrangle and the area in-between Tien River and Hau River.

2. The selection is based on the flood depths in "high stage" in floodplains (Hung et al., 2012): greater than 2 m depth, from 1 m to 2 m depth and below 1 m depth. The flood depths can be determined by intersection of inundation maps of different years derived from radar satellite images (Dung et al., 2011) and the digital elevation model (SRTM).

3. The sites should encompass full flood control compartments (termed "high dike" in Vietnam), as well as partial flood control compartment ("low dike"). For more information on the dike system see Hung et al. (2013a).

4. The sites should be suitable for a long flooding period monitoring.

Although each site should ideally include a low dike and a high dike, this criteria could not be met everywhere. High dike compartments do not exist everywhere, so that some sites contain low dike compartments only. Finally, 11 sites were selected containing 19 compartments (cf. Fig. 1, Table 1) with overall 11 low dike and 8 high dike compartments.

3 Sediment trap design and sampling scheme

Sedimentation is mostly monitored by sediment traps, as shown by a number of recent studies (Steiger et al., 2001, 2003; Middelkoop et al., 2005; Büttner et al., 2006; Hung et al., 2013b). Sediment traps can provide cumulative samples for different physical and chemical analyses. Flexible sediment traps are an adequate method for sampling sediment deposited by flowing water in floodplains and are in recent studies preferred to flat devices with a smoother surface, because they can represent the natural ground surface more appropriately (Steiger et al., 2003). We followed this recommendation and used flexible traps built from artificial grass with a rectangular dimension of 30 cm by 30 cm and 1.5 cm long tufts. The traps were fixed to the ground by bamboo stakes instead of steel pins, in order to avoid injuries of the farmers when they accidentally step on them in their fields.

HESSD
10, 325–373, 2013

A case study in the Mekong Delta

N. V. Manh et al.

Measurement of sedimentation using clusters of traps has been performed to indicate differences in sediment accumulation over short distances (Asselmann and Middelkoop, 1995), and to calculate average deposition rates (Steiger et al., 2001, 2003; Middelkoop et al., 2005). In the present study, in order to capture the representativeness of a single trap for the sedimentation processes of the monitoring location, small clusters of three traps were installed for every monitoring point (Fig. 2). By this repetition sampling, the variability at a given location can be captured. This variability stems from the different floodplain processes, both natural and anthropogenic, influencing the deposition. The traps of each cluster were positioned in an equiangular triangle of 2 m side length (Fig. 2). Each cluster was marked with flags on high poles to indicate the fishing farmers the trap location.

To be able to retrieve the traps from still ponding water with minimum sediment loss, the traps were designed with eight strings (60 cm long) attached to the corners and the middle of the sides. The traps were tested to withstand more than 60 $kg\,m^{-2}$, which is well above the maximum documented deposition of 20 $kg\,m^{-2}\,a^{-1}$ in MD (Hung et al., 2013b). When the traps are pulled up by the strings, they form a bowl-shape retaining most of the sediment (Fig. 3). However, the retrieval cannot be loss free, and it has to be expected, that the higher the deposition volume, the higher is the loss, as the overflow over the sides of the bowl is likely to carry more sediment compared to small deposition volumes. The loss due to retrieval is quantified by lab experiments presented in Sect. 5.1.

To quantify the spatial variability of deposition within a compartment, each compartment was equipped with several monitoring point clusters, each consisting of three traps. The monitoring points are arranged perpendicular and parallel to the expected flow direction in the compartment.

A total number of 149 measurement clusters (447 traps) were deployed at the monitoring sites for the measurement campaign starting in late July 2011 and lasting until mid-December 2011. The maximum and minimum number of points in a compartment were 14 and 5, respectively, while the biggest and the smallest monitored

HESSD
10, 325–373, 2013

compartments are 858 ha and 52 ha, respectively. The distance from the sites to main rivers range from 5 km in Dinh An compartment up to 71 km in Kien Binh 2 compartment (Table 1). The traps were retrieved just after the flood season and before cropping activities in the fields started. A large number of traps was lost or damaged, both due to the exceptionally high flood in this year (MRC, 2011), and fishing activities in the floodplains. The farmers owning the land where the traps were installed were informed and paid for taking care. However, during the flood season in the VMD the inundated land has legally no owner and everyone can fish everywhere, which partly explains the loss of some traps, as not everybody could have been informed about the monitoring activities. An overall number of 161 traps could be collected and used for laboratory analysis, which is equivalent to 38 % of all installed traps.

4 Monitoring results

The 161 traps represent 49 clusters of two or three traps and 26 single trap clusters, where the other traps were lost or destroyed. The deposition masses were measured after drying in a laboratory. Due to the assumption of small variability of physical and chemical sediment properties in the MD floodplains, 61 representative samples distributed in 12 compartments, including partially destroyed samples with sufficient volume, were analyzed for particle size distribution (sand, silt and clay fractions), pH, Total Nitrogen fraction (TN), Total Phosphorus fraction (TP), Total Potassium fraction (TK), and Total Organic Carbon fraction (TOC). The nutrient analysis provided proportional figures to the sediment masses. The analysis methods are described in Table 2.

Figure 4 presents the analysis results and their overall variability for all analyzed samples in box-whisker-plots. Sediment masses show a high variability with minimum and maximum deposition of 80 g and 1950 g respectively, while the median deposition is 500 g. This high variation is expressed in a high coefficient of variation of 0.64. The variability of the nutrient fractions is considerably lower. Minimum and maximum values are always in the same order of magnitude, and the coefficients of variation are 0.36,

HESSD
10, 325–373, 2013

0.21, 0.28 and 0.44 for TN, TP, TK and TOC, respectively. This finding supports the hypothesis that the nutrient content of the sediment is relatively uniformly distributed over the delta and that the spatial differences in nutrient input to the floodplains is mainly controlled by the deposition masses, and only to a minor extent by variable nutrient content of the sediments.

For pH extreme values up to 3.2 and slightly alkaline samples are observed. The grain size distribution is dominated by the silt and clay fractions with only little and sporadic sand components, as the low percentages and high number of outliers of the sand fraction showed. The coefficients of variation are 0.2, 0.22, 0.17 and 1.53 for silt, clay, pH and sand respectively. This is typical for suspended sediment in the MD (Wolanski et al., 1995; Thuyen et al., 2000; Hung et al., 2013a).

Figure 5 shows the variability of every of the 49 sample clusters for deposition mass derived from the sampling repetitions, and for the 12 compartment-wise collected samples for the remaining parameters. The different data aggregation levels, i.e. trap cluster for deposition mass and compartments for the remaining parameters, acknowledge the higher variability of the deposition mass and the quantification of the remaining parameters in relative terms, which is to a large extent independent of the actual deposition mass at a single monitoring point. For all parameters mean, standard deviation SD, and coefficient of variation CV are plotted. The clusters, compartment samples are sorted according to the mean. The standard deviations are always smaller than the mean resulting in CV below 1. The deposition mass data show an interesting trend in declining CV with mean deposition, indicating that the sampling uncertainty is smaller with higher deposition masses. This can be explained by the fact that even little disturbances can have a large effect on deposition in case of only small deposition volumes. For all other parameters besides deposition mass except the sand fraction, the variation within the compartments is comparatively low, as the small CV indicate (Fig. 5). This corroborates the finding that the nutrient content shows only little spatial variation, both within compartments and over the complete sampled domain. These findings imply that (a) an uncertainty analysis should be performed, and (b) that the focus should be laid on the

HESSD
10, 325–373, 2013

uncertainty in deposition mass, as this also influences the uncertainty in the estimation of absolute nutrient deposition.

5 Uncertainty analysis

5.1 Uncertainty associated to trap collection in ponding water

Trap removal from ponding water will always produce less (or equal at best) sediment mass compared to dry trap collection. Sediments can only be lost, not gained by trap removal from ponding water, as water flowing from the trap will carry parts of the deposited sediment when the trap is pulled out of the water. In order to quantify this loss, experiments were conducted in a small reservoir, where traps with known dry weight were pulled out of the water. The remaining sediment mass was determined by weighing after drying of the removed samples. The tests were performed with 7 different initial sediment masses equivalent to reported annual deposition masses of $0.3/20\,\mathrm{kg\,m^{-2}\,a^{-1}}$ (Hung et al., 2013b). The results of this test are shown in Fig. 6.

The data shown in Fig. 6 implies an exponential behavior. However, according to the constraint that the wet collection mass cannot be higher than the dry collection mass, a description of the data with an exponential model is difficult. Due to the proximity of the data to the constraint line, an exponential model not violating this constraint could not be found. Therefore the data were described by two linear models with a separating threshold of 620 g wet deposition mass:

The model 1: $y = 1.02x + 21.01 \quad \text{if} \quad x < 620$ (1)

The model 2: $y = 2.31x - 770.1 \quad \text{if} \quad x \geq 620$ (2)

With constraint: $y \geq x$ (3)

In which: x: Wet retrieval sediment mass (gram), y: Dry retrieval sediment mass (gram).

The 90 % Confidence Interval (CI), also shown in Fig. 6, is computed as CI = para $\pm\, t\sqrt{S}$, in which para denotes the estimated parameters, t depends on the confidence

Discussion Paper | Discussion Paper | Discussion Paper | Discussion Paper |

HESSD

10, 325–373, 2013

A case study in the Mekong Delta

N. V. Manh et al.

Title Page
Abstract Introduction
Conclusions References
Tables Figures
◀◀ ▶▶
◀ ▶
Back Close
Full Screen / Esc
Printer-friendly Version
Interactive Discussion

level, and is computed using the inverse of Student's t cumulative distribution function, and $\boldsymbol{S}$ is a vector of the diagonal elements from the estimated covariance matrix of the coefficient estimates (Mendenhall et al., 2009).

The use of two different models to describe the data can also be justified by the trap removal procedure. When the traps are removed by the strings, the mat forms a bowl-like shape. When there is only little sediment in the trap and the trap is removed carefully, only little sediment is re-suspended by the outflowing water. However, at a certain threshold the deposition mass is close to the brim of the "removal bowl", thus causing higher losses by the outflowing water or even direct losses in extreme cases. This threshold is experimentally determined by the step in losses shown in Fig. 6. There is some uncertainty in this threshold, as no data for deposition masses around 700 g is available. This uncertainty is captured by the confidence intervals. In the following this uncertainty is called "wet-dry correction model". This uncertainty source represents an epistemic uncertainty source according to the Merz and Thieken (2005).

5.2 Deposition uncertainty

The second uncertainty source of the sampling scheme is the deposition uncertainty, i.e. the representativeness of a sediment trap in view of small scale variability. This is an aleatory uncertainty source. The layout in clusters of three traps aimed at the quantification of this uncertainty. For every cluster with 2 or 3 three samples the mean and standard deviation as given by Fig. 5 were taken as a measure for the deposition uncertainty. Of course, the statistical significance of these moments is very limited due to the small sample size. However, given the constraints in sample numbers and analysis, we regard the information derived from the 3-sample clusters as an important step towards quantification of sediment deposition uncertainty, as already this small sample size indicates a large variability.

HESSD
10, 325–373, 2013

5.3 Monte Carlo analysis

The overall uncertainty stemming from variability in deposition and wet trap removal is quantified in a Monte Carlo (MC) framework. For every sampling location, the uncertainty from both sources is combined by randomized sampling of wet deposition and subsequent wet-dry sample mass correction. We assume normal distribution for the depositions over spatial units, as well as for the parameter uncertainty of the wet-dry correction model. Figure 4 shows that, with the exception of sand fraction, the data are not markedly skewed. It has to be noted that while the distribution of sand fraction is remarkably skewed over the study area, the distribution within a compartment unit resembles a normal distribution. The moments of the uncertainty distribution of the wet-dry correction model parameters are derived from the uncertainty bounds shown in Fig. 6.

The MC uncertainty analysis was performed for deposition mass, nutrient fractions (TN, TP, TK, TOC), grain size fractions (Sand, Silt, Clay) and pH. The uncertainty of the deposition mass was calculated for every monitoring point. This uncertainty was further propagated to nutrient masses by combining the deposition uncertainty with the uncertainty of the nutrient fractions. The grain size fraction and pH do not depend on the deposition mass, as the very small CV values indicate, thus the spatial units of their uncertainty analysis are the compartments.

According to the different spatial units, the uncertainty analysis consists of three workflows (shown in Fig. 7): uncertainty analysis for sediment mass, nutrient fractions, and finally grain size fractions and pH. The sediment mass workflow contains 2 branches: cluster traps and single traps. Details are given in the next section. For every parameter 5000 MC runs were performed.

5.3.1 Sediment mass uncertainty analysis

For the uncertainty analysis of sediment mass 34 clusters of three traps and 15 clusters of two traps were evaluated:

HESSD
10, 325–373, 2013

- *Step 1:* PDFs of cluster traps and single traps

  Cluster traps: MC sampling of the cluster trap data based on the mean and SD of each cluster trap.

  Single traps: MC sampling of single trap data taking the measured value as mean, based on the assumption that the measurement value is a good estimator of the (unknown) cluster mean. Single trap SD is derived from the SDs and the means of cluster traps by:

  - Fit a linear regression to cluster means versus cluster SDs (Fig. 8).
  - Calculate the 90 % CI for the fitted regression.
  - Take the upper 90 % CI as SD for the single trap cluster.

  By this procedure, it is ensured that (a) the observed reduction in CV with higher deposition mass (see Fig. 5) is taken into account, and (b) that the single trap values are considered more uncertain than the multiple trap clusters, because the upper 90 % CI of SD is in most cases higher as the SDs of the multiple trap clusters (Fig. 8).

- *Step 2:* Uncertainty in wet-dry correction models

  Calculate the dry deposition mass with Eqs. (1) or (2), where the parameters are randomly perturbed with the fitted value as mean, and SD derived from confidence intervals assuming a normal distribution.

- *Step 3:* Correct calculated deposition mass

  Truncate the results from step 2 according to the constraint given in Eq. (3).

- *Step 4:* Uncertainty bounds for sediment mass

  Construct the 90 % CI from the MC results of step 3 for every monitoring point.

HESSD
10, 325–373, 2013

5.3.2 Nutrient fraction

The laboratory results of nutrient analysis provide proportions of sediment mass (%). This means that the uncertainty of nutrient data is related to the sediment mass and its uncertainty. Moreover, the coefficient of variation of nutrient data is comparatively low, as well as the correlation coefficients between sediment mass and nutrient proportion. This implies that the nutrient compounds in sediment are approximately homogeneously distributed over the study area. Therefore, the uncertainty of the nutrient fractions can be calculated over a wider spatial unit and the nutrient mass and uncertainty calculation is based on the sediment mass calculations (step 1–4):

– *Step 5:* PDFs of nutrient fractions

  MC sampling for nutrient fractions based on the mean and SD of nutrient fraction calculated over the whole study area.

– *Step 6:* PDFs of nutrient mass

  Transform the nutrient fractions into nutrient mass by multiplying the results in step 5 with the result in step 3.

– *Step 7:* Uncertainty bounds for nutrient mass:

  Construct the 90 % CI of the PDFs results in step 6.

5.3.3 Grain size fraction and pH

In order to account for the observed differences in substrate and pH in the MD, the uncertainty of grain size distributions and pH is calculated compartment-wise. Variations in pH may well be caused by local redistribution of sediments. The acidic soils, e.g. in the Plain of Reeds, may influence pH and by pH based flocculation processes also the grain size distribution. Hence, the uncertainty of these parameters is evaluated for every monitored compartment, by calculating the statistical moments from compartment aggregated sample sizes.

HESSD
10, 325–373, 2013

– *Step 8:* PDFs of grain size fractions and pH

  MC sampling of those data based on compartment-means and SD

– *Step 9:* Uncertainty bounds for grain size fraction and pH

  Construct the 90 % CI of the PDFs results in step 9.

The results in step 4, 7, 9 are the uncertainty estimates of sediment mass, nutrient masses, pH and grain size fractions in terms of 90 % confidence intervals, which will be discussed in the next section.

6 Results and discussion

6.1 Varying uncertainty in datasets

In this section the differences in the derived uncertainty estimates from steps 4, 7, and 9 are discussed. Figure 9 shows the mean and 90 % CI of deposited sediment mass before and after the MC analysis, sorted by the measured mean original deposition mass. It can be seen that the uncertainty bounds can be very large, and that there is a trend towards higher uncertainty with higher sediment mass. In cases where a high deposition mass, i.e. a high uncertainty stemming from the extraction of the samples from ponding water meets high deposition uncertainty derived from the trap clusters, the upper 90 % CI can be up to almost twice the mean. If the deposition uncertainty is low, the overall uncertainty is also well contained in narrow CI's. The lower CI is closer to the mean and smoother due to the constraint in the wet-dry-sampling correction. With smaller original measured sediment mass, the uncertainty is smaller in absolute terms as the wet-dry-sampling uncertainty is lower (cf. Sect. 5.1).

The threshold for the two wet-dry correction models is also reflected in Fig. 9 by a widening of the CI above the threshold, as expected. As this threshold is related to the size of the traps, it can be concluded that the trap size (sampling area covered) should be as large as possible in order to reduce the wet-dry correction uncertainty. From general considerations on local re-suspension and relocation of deposited sediment, it is expected that also the sampling uncertainty will also reduce with increasing trap size.

The uncertainty bounds of deposited nutrients ($g\,m^{-2}$) are propagated from sediment weight bounds based on the analyzed nutrient fractions (%). Therefore, the uncertainty bounds show the same characteristics as for the sediment masses (Fig. 10). Due to the additional uncertainty of the nutrient fraction, the relative uncertainty is increased for the nutrient deposition estimates. These features become more obvious in Fig. 11 showing the CI's of the sediment and nutrient deposition relative to the mean values. The smallest and largest relative uncertainty belongs to sediment mass and TOC, respectively. Overall, the variability of the upper uncertainty bounds ranges from 20 % to 100 % of the mean, while the lower uncertainty bounds are 20 %–50 % lower than the mean. The deposition mass threshold between the two wet-dry correction models is also clearly visible in Fig. 11 showing a step change in the uncertainty bounds, as illustrated by the linear regression lines. The range of the bounds in the sediment and nutrient deposition mass below the threshold are 60 % and 30 % for the upper and lower bound, respectively, while the range above the threshold are 80 % and 45 % for the upper and lower bound. As this feature is a direct consequence of the applied wet-dry correction models, it can be inferred that a larger range of deposition masses in laboratory tests for the correction could result in a continuous correction model and consequently the step change in the uncertainty bounds could be removed. However, as the step change has physical causes related to the deposition volume and trap size, this is not guaranteed.

In contrast to the nutrients, the grain size fractions and pH show different uncertainty characteristics, as they do not depend on the deposition mass (Fig. 12). The confidence intervals are small compared to sediment mass and nutrients and essentially symmetric, which is a consequence of the assumption of normal distributed deposition uncertainty. The sand fraction has the highest uncertainty for large sand fraction values, illustrating the sporadic and most likely locally influenced sand content of the

HESSD
10, 325–373, 2013

suspended sediments in the VMD. The opposite holds true for the clay fraction, where the uncertainty is highest for low clay fractions. This effect has to be attributed to the small particle size and the related sensitivity of the laboratory analysis of the clay fraction.

In relative terms the uncertainty bounds of grain sizes and pH generally range from 10 % to 50 % with the exception of the sand grain size fraction, which can be as large as 150 % (Fig. 13). This makes the sand fraction the most uncertain component in this analysis, followed by the clay fraction when the mean is below 30 %. A ranking according to overall uncertainty is given in Table 3.

6.2 Sedimentation rates and nutrient sediment rates

Across the study sites, the sedimentation rate in the MD varied from 1.9 $kg\,m^{-2}\,a^{-1}$ to 44.9 $kg\,m^{-2}\,a^{-1}$, equivalent to 1.6 $mm\,a^{-1}$ to 37.4 $mm\,a^{-1}$, and the mean equals 9.5 $mm\,a^{-1}$. The nutrition rates are proportional to the sedimentation rate at the monitoring points. TOC has the biggest rate, the maximum rate is close to 2300 $kg\,m^{-2}\,a^{-1}$ and the mean rate is about 660 $kg\,m^{-2}\,a^{-1}$. The mean rates of TN, TP and TK are 46 $kg\,m^{-2}\,a^{-1}$, 17 $kg\,m^{-2}\,a^{-1}$, and 210 $kg\,m^{-2}\,a^{-1}$, respectively. Table 4 provides an overview of the sedimentation rates over all study sites. Differentiating the results in low and high dike compartments, it can be shown that the maximum sediment and nutrient deposition in low dike compartments doubles the maximum rate in high dike compartments (Table 4). Also the minimum values are more extreme in the low dike compartments. However, the average values are 11.6 $kg\,m^{-2}\,a^{-1}$ and 10.6 $kg\,m^{-2}\,a^{-1}$ in low and high dike system, respectively. This indicates that on average no significant difference between low and high dike systems could be observed, but the variability in deposition is considerably higher in the low dike compartments (1.9 $kg\,m^{-2}\,a^{-1}$/49.9 $kg\,m^{-2}\,a^{-1}$) compared to the high dikes (4.5 $kg\,m^{-2}\,a^{-1}$/19.8 $kg\,m^{-2}\,a^{-1}$). This is a consequence of the different hydraulic links between the channels and the floodplains of the different dike systems. However, in the interpretation of these results the severity of the flood in

HESSD
10, 325–373, 2013

2011 has to be taken into account. The high flood peak and long inundation duration reduced the differences in floodplain inundation between the two dike systems.

The differences in grain size distribution between low and high dikes are little, although there is a slight tendency that the low dike compartments exhibit a higher overall variability (Table 4). This can be explained by the generally higher flow in the low dike compartments, which are hydraulically fully connected to the channels, whereas the flow in the high dike compartments is controlled and limited by the sluice gate capacities.

The low pH values in Table 4 can explained by the acid sulphate soils found in large parts of the MD floodplains. The total acid soil area is 1.1×10^6 ha over total 1.8×10^6 ha in floodplain area, i.e. about 60 % of the floodplains have acid soils (Soil map – MONRE[1]). Moreover, the extraordinary inundation duration in 2011 with strong influence of re-suspension processes might have caused a further reduction in pH in sediment samples.

In order to compare and interpret these figures a comparison with six major rivers in South East Asia is conducted (Table 5). The Mekong River is the third largest and longest river, and fifth and fourth in terms of sediment flow and total dissolved solid (Milliman et al., 2011). The average suspended sediment concentration (SSC) in the MD and the Yangtze Delta is approximately identical in terms of maximum monthly SSC, and much smaller than those in the Red River and Yellow River. The silt and clay grain fractions account for more than 90 % with an average of about 40 % clay. This is equivalent to published data of the Yangtze Delta. The similarities between the Mekong and the Yangtze might me partially explained by their shared origin in the Tibetan plateau.

A comparison of floodplain sedimentation in these deltas is difficult as hardly any data are available. However, a comparison with the published sedimentation rate in the Yangtze Delta shows that the average sedimentation rate in the MD is similar to the

[1] Ministry of Natural Resources and Environment.

HESSD
10, 325–373, 2013

result in the Yangtze Delta, but showing a larger variability. This can be interpreted as an impact of the intensive fragmentation of floodplains in the MD.

6.3 Spatial variability of sedimentation

The spatial distribution of floodplain sedimentation is controlled by the channel and dike systems in the VMD. The channel system is classified as follows: The main channels are “large” channels conveying floods from Tien River and Hau River through the Delta and the associated dikes are typically combined with provincial roads (high dikes). The secondary channels are “medium” channels branching from the main channels and creating compartments (high dikes or low dikes). Within these large compartments inner “small” channels exist. These channels are used for agricultural transportation and drainage, and are accompanied by low dikes, if at all.

Normally, a compartment in the Mekong floodplains consists of a secondary ring channel accompanied with high dikes or low dikes, some inner channels with its banks, sluice gates, open culverts, and pumping stations. The flood water from the rivers flows into the channel network and is then redistributed into compartments through hydraulic structures for high dike systems or overflows into compartments in “high stage” in low dike systems (Hung et al., 2012). The sediment movement into compartment includes advective transport with flow (primary transportation) and an additional but small dispersive component. This means that theoretically the low dike compartments potentially have a higher chance to receive a higher sedimentation than the high dike, as the flow into the compartment is less restricted and the flow velocity is higher on average. However, as this and a previous study (Hung et al., 2012) indicate, a clear distinction of the floodplain sedimentation between the different dike systems cannot be found. The complex interplay of inundation dynamics, channel and dike systems, and the high number of hydraulic structures creates a differentiated sedimentation pattern without obvious correlations or patterns.

A spatial interpolation of the derived sedimentation data is thus not performed over the whole VMD, but compartment wise. Inverse Distance Weighting (IDW) interpolation

HESSD
10, 325–373, 2013

was applied on the mean values. Figure 14 shows exemplarily the Phu Thanh site. Both compartments are located in the center of a main channel ring with a lot of secondary channels and inner channels. The mean sedimentation rate in the high dike O Bao 18 compartment (14.4 $kg\,m^{-2}\,a^{-1}$) is significant higher than that in the nearby low dike Phu Hoa compartment (6.3 $kg\,m^{-2}\,a^{-1}$). Also the spatial variability within the compartment is in this case higher in the high dike compartment than in the low dike compartment. This seems to be contradictory to the postulated higher general variability in low dike compartments, but can be explained by the fact that locally, i.e. in a compartment, the spatial deposition in high dike compartments is influenced to a large extent by the position and operation of the sluice gates. From these results of these two compartments a slight trend towards lower deposition in the center of the floodplain between the main channels could be postulated, but as data from the surrounding compartments are missing, this cannot be corroborated.

A similar result can be found in the Kien Binh site (Fig. 15), where a high dike system in Khu Tram Bom compartment and a low dike in Bay Thuoc compartment weres monitored. Both compartments are located next to a main channel, but have different sediment sources that lead to be completely different sedimentation patterns and values. The average sedimentation rate in Khu Tram Bom compartment is 8.7 $kg\,m^{-2}\,a^{-1}$ and much smaller in Bay Thuoc compartment 2.6 $kg\,m^{-2}\,a^{-1}$. It can be seen, that higher sedimentation rate is in closer distance to sediment sources, i.e. the sluice gates connecting the floodplain to the main and secondary channels.

Figure 16 shows the interpolated deposition in My Hiep Son compartment. This is a typical pattern of high variability of sedimentation rates in low dike systems. The values of maximum and minimum rates are 4.1 $kg\,m^{-2}\,a^{-1}$ and 32.8 $kg\,m^{-2}\,a^{-1}$, respectively, compared to the average rate of 16.1 $kg\,m^{-2}\,a^{-1}$. On one hand, the CV of sedimentation rates equal 0.5 in My Hiep Son compartment which is significantly higher than CVs in high dike compartments. On the other hand, the higher sedimentation rates are related to the better hydraulic linkage to the main channel.

HESSD
10, 325–373, 2013

In summary, the fragmentation of the floodplains by the channel and dike systems destroyed the natural consistency and continuity of the MD floodplains. Table 6 shows the mean values of sedimentation in different larger spatial units, i.e. regions of the VMD. In this analysis, the Long Xuyen Quadrangle receives a higher mean sediment deposition as the Plain of Reeds. However, the deposition within high dike compartments is on the mean comparable between the two regions, but the monitored low dike compartments receive considerably less sediments in the Plain of Reeds, explaining the differences in the overall deposition Interestingly, if averaged over the whole study regions, the mean deposition in high and low dikes is again comparable. An interesting aspect of this analysis is that over the whole VMD the deposition in low dike compartments shows a higher variability, i.e. varies higher between the regions of the VMD, but within compartments the spatial variability is higher in the high dike compartments as a consequence of the concentration of sediment sources to the locations of the sluice gates.

7 Conclusions

This study proposes a procedure to monitor quantity and spatial variability of sediment and associated nutrient deposition in large and complex river floodplains including an uncertainty analysis. The uncertainty estimation consists of (1) sediment trap design and trap retrieval from still inundated floodplains, (2) trap installation in clusters to quantify the uncertainty due to local variability, (3) trap retrieval test to quantify losses by sample collection from inundated floodplains, and (4) a Monte Carlo framework for estimating uncertainty bounds.

This methodology is applied to the Vietnamese Mekong Delta. The 90 % uncertainty interval of the sediment deposition mass is less than 100 % of the mean values for the entire dataset. The nutrient deposition uncertainty is slightly larger, as it directly depends on the sedimentation mass, but the determination of the nutrient content adds another uncertainty source. The uncertainties associated to grains sizes and pH are

HESSD
10, 325–373, 2013

considerably smaller, as they are hardly affected by uncertainties in deposition mass. In contrast to the sediment deposition mass, these properties generally do not show a large spatial variation. The sand fraction is the only exception in this respect. This finding can be attributed to the fact that the sand fraction in floodplain deposits is generally low and highly influenced by local relocation processes. The sediment source, i.e. the suspended sediment in the MD, contains only a very small sand fraction.

The main uncertainty sources are the trap retrieval from still inundated floodplains and likely human interference on the floodplains and floodplain inundation. While the sediment retrieval uncertainties are systematic and quantifiable, the variability caused by human interference and small scale differences in deposition and re-suspension is an aleatory uncertainty, which is difficult to attribute to distinct factors. Human interference ranges from direct impact on the sedimentation, by e.g. disturbances, by fishing on the floodplains with nets, to indirect causes by regulating floodplain inundation by sluice gate control and operation of pumps. Human interference will remain a large uncertainty source, unless strictly centralized and enforced regulations of operation of hydraulic structures are implemented. For the monitoring of floodplain inundation local actions to restrict fishing activities could help, although this is almost impossible to enforce.

Mean sediment deposition values are highly variable, both for the whole set of monitoring points and among the different compartments. The variability among the compartments cannot be attributed to the dike system (low crop protection dikes or high flood protection dikes), as the differences in mean deposition is negligible. However, deposition in low dike compartments showed a higher variability compared to the high dike compartments if analyzed over the whole VMD, indicating the normalizing influence of the controlled floodplain inundation in the high dike compartments. In contrast to these findings, the spatial variability within individual compartments tends to be higher in high dike compartments, as the sediment source as well as the flow in the compartments are controlled by the location and operation of the sluice gates. Both source and flow can be assumed to be more homogeneous in low dike compartments

HESSD
10, 325–373, 2013

leading to less spatial variability of in-department deposition. A larger influence on floodplain deposition seems to be caused by the distance to the main channels and the location and number of sluice gates.

All findings have to be interpreted in combination with the extraordinary flood in the study year 2011, for which peak flow and duration were the second largest in the observation period of about 80 yr. Hence, the observed sedimentation may not be representative for the typical flood situation in the VMD. We expect that during normal flood years the differences between the low and high dike systems are more pronounced. Therefore, a repetition of the measurement campaign would not only provide additional statistical significance to the presented results, but potentially also yield a better understanding of the impact of the dike systems on floodplain sedimentation in the VMD.

Because of the observed low spatial correlation of the floodplain sedimentation, an interpolation of the point samples to large scale sedimentation is not feasible. The derived data are lacking the required autocorrelation and meaningful variograms for geostatistical interpolation. Potentially, a large scale spatial estimation of floodplain deposition could be derived via remote sensing. Optical satellite products can quantify suspended sediment concentrations, from which the deposition could be inferred. The problem with this approach is the high cloud cover during the flood/monsoon period. Therefore, a spatial estimation of floodplain sedimentation has to rely on numerical simulation of the floodplain hydraulics and deposition processes, for which the derived data and uncertainty estimates can provide the required calibration data. Consequently this will be the next step in our analysis of the floodplain sedimentation of the VMD.

Acknowledgements. The presented work was performed within the project WISDOM – Water related Information System for a Sustainable Development of the MD (www.wisdom.eoc.dlr.de). Funding by the German Ministry of Education and Research BMBF and the Vietnamese Ministry of Science and Technology is gratefully acknowledged.

The service charges for this open access publication have been covered by a Research Centre of the Helmholtz Association.

References

Asselman, N. E. M. and Middelkoop, H.: Floodplain sedimentation: quantities, patterns and processes, Earth Surf. Proc. Land., 20, 481–499, 1995.

Basil, M.: Uncertainty of complex systems by Monte Carlo simulation, North Sea Flow Measurement Workshop, October 1998, 26–29, 1998.

Büttner, O., Otte-Witte, K., Krüger, F., Meon, G., and Rode, M.: Numerical modelling of floodplain hydraulics and suspended sediment transport and deposition at the event scale in the middle river Elbe, Germany, Acta Hydroch. Hydrob., 34, 265–278, 2006.

Datta, D. K. and Subramanian, V.: Texture and mineralogy of sediments from the Ganges-Brahmaputra-Meghna river system in the Bengal Basin, Bangladesh and their environmental implications, Environ. Geol., 30, 181–188, 1997.

Dung, N. V., Merz, B., Bárdossy, A., Thang, T. D., and Apel, H.: Multi-objective automatic calibration of hydrodynamic models utilizing inundation maps and gauge data, Hydrol. Earth Syst. Sci., 15, 1339–1354. doi:10.5194/hess-15-1339-2011, 2011.

Funabiki, A., Haruyama, S., Quy, N. V., Hai, P. V., and Thai, D. H.: Holocene delta plain development in the Song Hong (Red River) delta, Vietnam, J. Asian Earth Sci., 30, 518–529, 2007.

Hung, N. N., Delgado, J. M., Tri, V. K., Hung, L. M., Merz, B., Bárdossy, A., and Apel, H.: Floodplain hydrology of the Mekong Delta, Vietnam, Hydrol. Process., 26, 674–686, doi:10.1002/hyp.8183, 2012.

Hung, N. N., Delgado, J. M., Guentner, A., Merz, B., Bardossy, A., and Apel, H.: Sediment in the floodplains of the Mekong Delta, Vietnam Part I: suspended sediment dynamics, Hydrol. Process., in review, 2013a.

Hung, N. N., Delgado, J. M., Guentner, A., Merz, B., Bardossy, A., and Apel, H.: Sediment in the floodplains of the Mekong Delta, Vietnam Part II: deposition and erosion, Hydrol. Process., in review, 2013b.

Li, G., Wei, H., Han, Y., and Chen, Y.: Sedimentation in the Yellow River delta, Part I: Flow and suspended sediment structure in the upper distributary and the estuary, Mar. Geol., 149, 93–111, 1998.

Liu, J. P., Li, A. C., Xu, K. H., Velozzi, D. M., Yang, Z. S., Milliman, J. D., and DeMaster, D. J.: Sedimentary features of the Yangtze River-derived along-shelf clinoform deposit in the East China Sea, Cont. Shelf Res., 26, 2141–2156, 2006.

HESSD

10, 325–373, 2013

A case study in the Mekong Delta

N. V. Manh et al.

Mekong River Commission: Origin, fate and impacts of the Mekong sediments, Techical report – MRC, available at: http://www.mpowernetwork.org/Knowledge_Bank/Key_Reports/Research_Reports/DMS_Sediments.html (last access: 7 January 2013), 2009.
Mekong River Commission: Flood Situation Report 2011, Technical Paper – MRC, 36, 2011.
Mendenhall, W., Beaver, R. J., and Beaver, B. M.: Introduction to Probability and Statistics, 13th Edn., Brooks/Cole, Cengage Learning: Belmont, CA, 308 pp., 2009.
Merz, B. and Thieken, A. H.: Separating natural and epistemic uncertainty in flood frequency analysis, J. Hydrol., 309, 114–132, 2005.
Middelkoop, H.: Floodplain Sedimentation – Methods, Patterns, and Processes, A Review with examples from the lower Rhine, the Netherlands, Hydrol. Sci., 7, HSA085, doi:10.1002/0470848944.hsa085, 2005.
Milliman, J. D.: River discharge to the coastal ocean: a global synthesis, Oceanography, 24, 143–144, doi:10.5670/oceanog.2011.108, 2011.
Navratil, O., Esteves, M., Legout, C., Gratiot, N., Nemery, J., Willmore, S., and Grangeon, T.: Global uncertainty analysis of suspended sediment monitoring using turbidimeter in a small mountainous river catchment, J. Hydrol., 398, 246–259, 2011.
Papadopoulos, C. E. and Yeung, H.: Uncertainty estimation and Monte Carlo simulation method, Flow Meas. Instrum., 12, 291–298, 2001.
Salas, J. D.: Uncertainty analysis of reservoir sedimentation, J. Hydraul. Eng., 125, 339–350, 1999.
Shamsudin, S., Rashid, A., Darom, M., Mohamad, I. N., Rahman, A. A., Campus, I., and Lumpur, K.: Detention pond sediment accumulation prediction using Monte Carlo simulation, Am. J. Environ. Sci., 8, 25–34, 2012.
Shenliang, C., Guoan, Z., and Shilun, Y.: Temporal and spatial changes of suspended sediment concentration and resuspension in the Yangtze River estuary, J. Geogr. Sci., 13, 498–506, 2003.
Steiger, J., Gurnell, A. M., Ergenzinger, P., Snelder, D., and Universita, F.: Sedimentation in the riparian zone of an incising river, Earth Surf. Proc. Land., 108, 91–108, 2001.
Steiger, J., Gurnell, A. M., and Goodson, J. M.: Quantifying and characterizing contemporary riparian sedimentation, River Res. Appl., 19, 335–352, 2003.
Tanabe, S. and Hori, K.: Song Hong (Red River) delta evolution related to millennium-scale Holocene sea-level changes, Quaternary Sci. Rev., 22, 2345–2361, 2003.

Thorne, C. R., Russell, A. P. G., and Alam, M. K.: Planform pattern and channel evolution of the Brahmaputra River, Bangladesh, Geol. Soc. London, 75, 257–276, 1993.
Thuyen, L., Tran, H., Tuan, B., and Bay, N.: Transportation and deposition of fine sediment during flood season in Long Xuyen Quadrangle, Technical Report – MOST (Vietnamese), 1–70, 2000.
Walling, D. E.: The changing sediment load of the Mekong River, Roy. Swed. Acad. Sci., 37, 150–157, 2008.
Wolanski, E.: Fine-sediment Dynamics in the Mekong River Estuary, Vietnam, Estuar. Coast. Shelf S., 43, 565–582, 1996.
Xue, Z., Liu, J. P., DeMaster, D., Van Nguyen, L., and Ta, T. K. O.: Late Holocene evolution of the Mekong subaqueous delta, Southern Vietnam, Mar. Geol., 269, 46–60, 2010.
Yang, S. L., Belkin, I. M., Belkina, A. I., Zhao, Q. Y., Zhu, J., and Ding, P. X.: Delta response to decline in sediment supply from the Yangtze River: evidence of the recent four decades and expectations for the next half-century, Estuar. Coast. Shelf S., 57, 689–699, 2003.
Yoshimura, C., Zhou, M., Kiem, A. S., Fukami, K., Prasantha, H. H. A., Ishidaira, H., and Takeuchi, K.: 2020s scenario analysis of nutrient load in the Mekong River Basin using a distributed hydrological model, Sci. Total Environ., 407, 5356–5366, 2009.

HESSD
10, 325–373, 2013

Table 1. Sediment trap installation and collection in 19 compartments, and distance from the sites to main rivers.

No	Compartment	Number of collected traps	Number of installed traps	Percent (%)	Distance to river
1	Vinh Thuan 1	9	15	60 %	50 km
2	Vinh Thuan 2	20	27	74 %	50 km
3	Kien Binh 1	15	15	100 %	70 km
4	Kien Binh 2	27	27	100 %	71 km
5	Phu Thanh B1	14	15	93 %	12 km
6	Phu Thanh B2	10	15	67 %	8 km
7	Phu Thanh B3	4	15	27 %	10 km
8	Ba Sao 1	2	24	8 %	15 km
9	Ba Sao 2	1	30	3 %	15 km
10	Phu Dien	1	24	4 %	40 km
11	Dinh An	2	24	8 %	5 km
12	Hoa Binh Thanh	6	36	17 %	7 km
13	Vinh An 1	2	15	13 %	20 km
14	Vinh An 2	1	27	4 %	21 km
15	Dao Huu Canh	20	42	48 %	15 km
16	My Hiep Son 1	17	24	71 %	47 km
17	My Hiep Son 2	17	33	52 %	40 km
18	Thanh Quoi 1	1	24	4 %	18 km
19	Thanh Quoi 2	2	15	13 %	18 km
		171	447	38 %	

HESSD
10, 325–373, 2013

N. V. Manh et al.

Table 2. Analysis methods for physical and chemical properties of sediment samples.

Analysis	Method
Mass	Drying and weighing in the laboratory
D	Robinson pipette method {sand > 0.063 mm > silt > 2 µm clay}
pH	pH meter: soil : water ratio 1 : 2.5
TN	Micro Kjeldahl: using H_2SO_4-$CuSO_4$-Se, ratio: 100-10-1
TP	Attacked by H_2SO_4-$HClO_4$ (1 : 5) desalinate phosphomolybdate by ascorbic acid, color comparison with Photometer.
TK	Attacked by HF-$HClO_4$ (10 : 1) Determine *K* by Atomic Absorption
TOC	Walkley-Black: oxidation by H_2SO_4-$K_2Cr_2O_7$, titrated by $FeSO_4$

HESSD
10, 325–373, 2013

Table 3. Uncertainty rank (sorted from low to high uncertainty) of sediment mass, nutrient mass, grain size fractions and pH. The uncertainty is expressed as 90 % CI of PDFs.

Rank	Parameter		Mean	Lower CI	Upper CI
1	pH (%)	min	3.9	−30 %	+7 %
		max	5.8	−7 %	+30 %
2	Silt (%)	min	40.7	−67 %	+2 %
		max	63.1	−2 %	+67 %
3	Clay (%)	min	31.4	−100 %	+8 %
		max	54.2	−8 %	+128 %
4	Sediment dep. rate (kg)	min	1.9	−7 %	+11 %
		max	44.9	−54 %	+97 %
5	TK (g)	min	33.4	−20 %	+31 %
		max	712.9	−55 %	+97 %
6	TN (g)	min	7.4	−23 %	+36 %
		max	158.1	−57 %	+103 %
7	TP (g)	min	2.8	−16 %	+26 %
		max	60.4	−54 %	+95 %
8	TOC (g)	min	107.0	−26 %	+42 %
		max	2268.3	−57 %	+108 %
9	Sand	min	0.8	−100 %	+54 %
		max	25.5	−54 %	+170 %

HESSD
10, 325–373, 2013

Table 4. Mean, median, minimum and maximum values of sediment and nutrient deposition rates over all study sites, and separated for low dike and high dike compartments.

		Sediment		TN	TP	TK	TOC	Sand	Silt	Clay	
		($kg\,m^{-2}$)	(mm)	($g\,m^{-2}$)	($g\,m^{-2}$)	($g\,m^{-2}$)	($g\,m^{-2}$)	(%)	(%)	(%)	pH
Overall	Min	1.9	1.6	7.4	2.8	33.8	107.8	0.8	40.7	31.4	3.9
	Median	8.4	7.0	34.4	13.2	158.3	501.1	2.7	51.2	40.7	4.9
	Mean	11.4	9.5	45.9	17.6	209.3	666.3	7	50.9	40.8	4.8
	Max	44.9	37.4	156.9	60.3	715.7	2296.5	25.5	63.1	54.2	5.8
Low dike	Min	1.9	1.6	7.4	2.8	33.8	107.8	0.8	40.7	31.4	4
	Median	7.4	6.2	30.6	11.9	140.4	449.1	2.5	50.7	41.3	5
	Mean	11.6	9.7	47.8	18.4	218.3	695.4	5.7	50.3	42.3	4.9
	Max	44.9	37.4	156.9	60.3	715.7	2296.5	21.4	58.5	54.2	5.8
High dike	Min	4.5	3.8	16.9	6.3	75	242.2	2.6	43.2	31.5	3.9
	Median	10	8.3	37	14.2	168.3	528.6	4.5	51.7	33.4	4.8
	Mean	10.6	8.8	39.6	15.1	180.2	572.6	10.8	52.7	36.1	4.7
	Max	19.8	16.5	72.3	27.7	330.1	1045.1	25.5	63.1	43.6	5.4

Discussion Paper | Discussion Paper | Discussion Paper | Discussion Paper |

HESSD

10, 325–373, 2013

A case study in the Mekong Delta

N. V. Manh et al.

Table 5. Sediment characteristics of some major rivers in South East Asia.

River	Length/Area km $(10^3\,km^2)^{-1}$	TDS/TSS $10^6\,t\,yr^{-1}$	Average of max monthly SSC	Grain size (%)	Sedimentation rate $(cm\,yr^{-1})$
Mekong	4800/800[a]	60/110(150)[a]	$0.326\,kg\,m^{-3}$ Tan Chau station	7 % sand, 51 % silt 42 % clay	0.16–3.7
Yangtze	6300/1800[a]	180/470[a]	$0.292\,kg\,m^{-3}$[b] Xuliujing station	5 % sand 40–45 % clay, 40–60 % silt[e]	1.4–2.5[h]
Yellow river	5500/750[a]	21/150 (1100)[a]	$34.7\,kg\,m^{-3}$[c] Lijin station	11.8 % clay, 79.4 % silt, 8.8 % sand[(3)]	
Ganges-Brahmaputra	2200/1650[a]	154/1060[a]		75–80 % silt[f] 17–37 % clay[g]	
Irrawaddy	2300/430[a]	98/325(360)[a]			
Red river	1100/160[a]	20/50(110)[a]	$1.08\,kg\,m^{-3}$[d] Hanoi station		

[a] Milliman et al. (2010), [b] Shenliang (2003), [c] Li (1998), [d] Tanabe et al. (2003c), [e] Liu (2006), [f] Thorne et al. (1993), [g] Datta and Subramanian (1996), [h] Yang (2003).

HESSD
10, 325–373, 2013

Table 6. Mean sedimentation values in different spatial units: compartments, low dike and high dike, Plain of Reeds/Long Xuyen Quadrangle and whole VMD.

<table>
<tr><th>No</th><th>Compartment</th><th colspan="9">Value (kg m^{-2})</th></tr>
<tr><td>1</td><td>Phu Thanh B2</td><td>6.3</td><td rowspan="3">low dike</td><td rowspan="3">8.0</td><td rowspan="6">Plain of Reeds</td><td rowspan="6">9.1</td><td rowspan="11">Overal the Mekong Delta</td><td rowspan="11">11.4</td><td rowspan="6">low dike</td><td rowspan="6">11.6</td></tr>
<tr><td>2</td><td>Kien Binh 1</td><td>2.7</td></tr>
<tr><td>3</td><td>Vinh Thuan 1</td><td>3.9</td></tr>
<tr><td>4</td><td>Vinh Thuan 2</td><td>10.2</td><td rowspan="3">high dike</td><td rowspan="3">10.8</td></tr>
<tr><td>5</td><td>Kien Binh 2</td><td>7.7</td></tr>
<tr><td>6</td><td>Phu Thanh B1</td><td>6.0</td></tr>
<tr><td>7</td><td>My Hiep Son 1</td><td>4.1</td><td rowspan="3">low dike</td><td rowspan="3">14.1</td><td rowspan="5">Long Xuyen Quad</td><td rowspan="5">13.6</td><td rowspan="5">high dike</td><td rowspan="5">10.6</td></tr>
<tr><td>8</td><td>My Hiep Son 2</td><td>5.8</td></tr>
<tr><td>9</td><td>Dao Huu Canh</td><td>44.9</td></tr>
<tr><td>10</td><td>Thanh Quoi 2</td><td>24.6</td><td rowspan="2">high dike</td><td rowspan="2">10.0</td></tr>
<tr><td>11</td><td>Hoa Binh Thanh</td><td>9.8</td></tr>
</table>

HESSD
10, 325–373, 2013

HESSD
10, 325–373, 2013

A case study in the Mekong Delta

N. V. Manh et al.

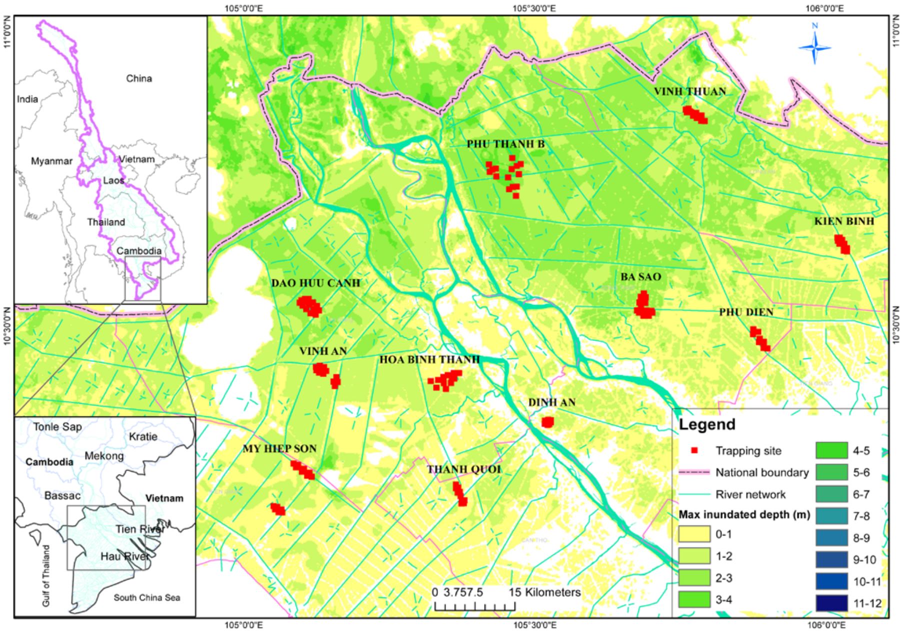

Fig. 1. The study area in the MD in Vietnam: the main map shows the mean of maximum observed inundation depths over 2000/2010 period, and the 11 selected sites including 19 compartments of either high dike or low dike systems. The map top left shows the entire Mekong River Basin and the map bottom left shows the entire MD.

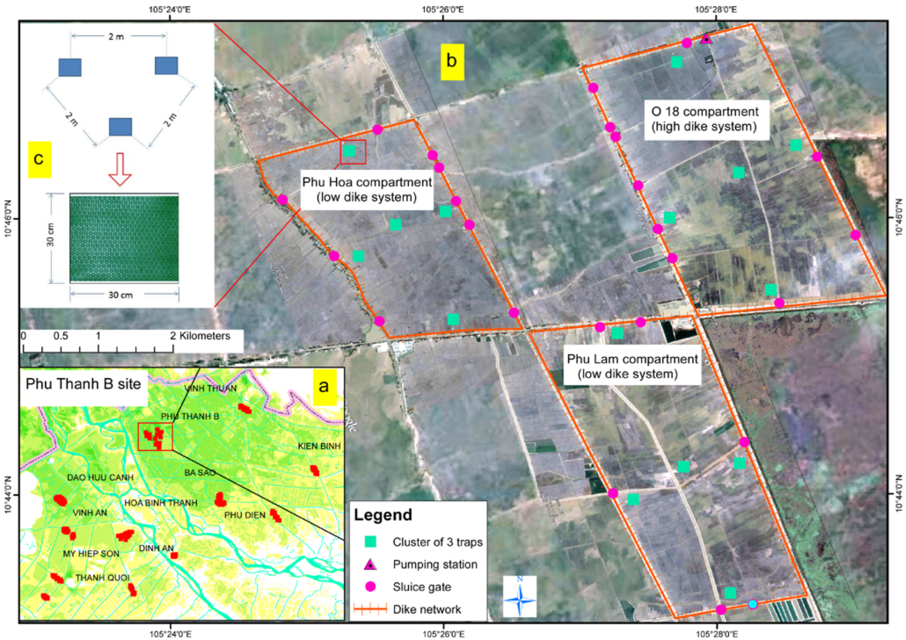

Fig. 2. Map illustrating the typical setup of the sediment traps in a site: map **(a)** shows all selected sites. The main map **(b)** describes the sediment trap installation in the study site of Phu Thanh B, the map **(c)** shows a cluster of 3 traps, the distances between the traps and the dimension of a trap.

HESSD
10, 325–373, 2013

Fig. 3. The sediment trap design, strength and balance test. Left: a fixed trap on the ground, right: bowl-shape trap when pulled up.

HESSD
10, 325–373, 2013

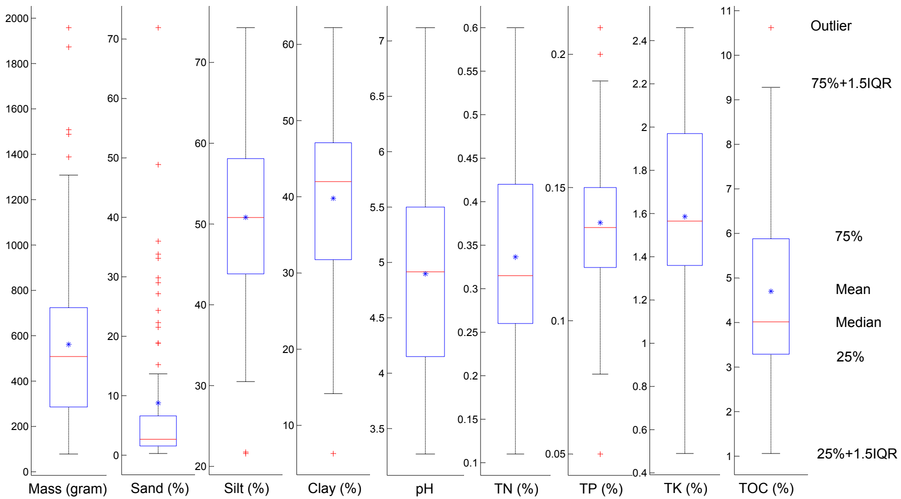

Fig. 4. Box plots of all data: sediment mass (*g*), sediment grain size classification of Sand, Silt and Clay (%), potential Hydrogen (pH), Total Nitrogen (TN) (%), Total Phosphorus (TP) (%); Total Potassium (TP) (%) and Total Organic Carbon (TOC) (%).

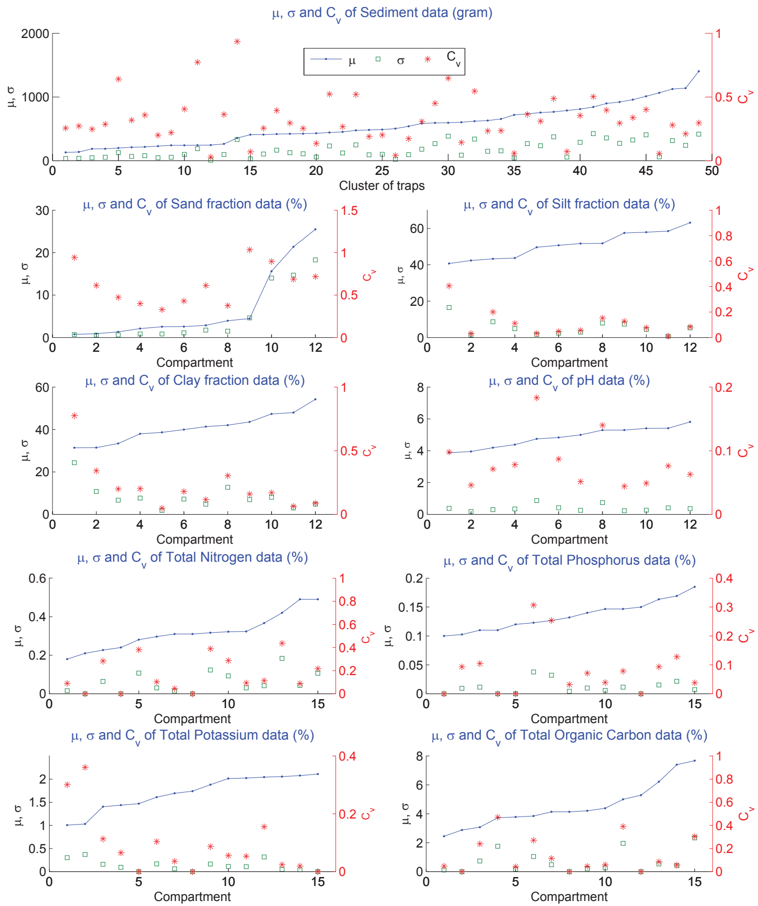

Fig. 5. The means (μ), standard deviations (σ) and coefficient of variation (V) of sediment weight on cluster traps, pH and nutrient data in compartments.

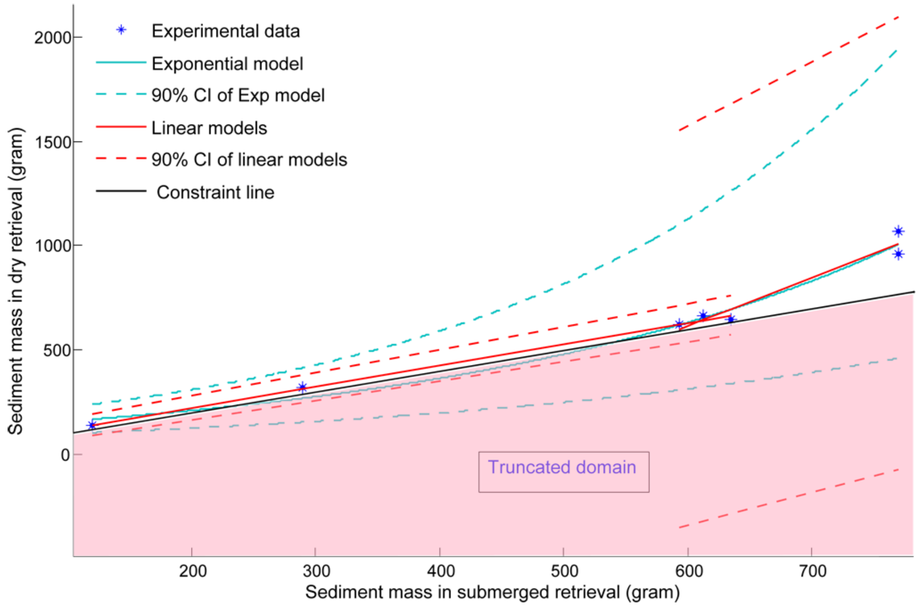

Fig. 6. Experimental results of trap retrieval from ponding water and under dry condition. The blue stars are the experimental data, the red lines are the linear regression models and their 90 % confidence intervals, and the cyan lines are an exponential regression model and its 90 % confidence intervals. The truncated domain is the area below the constraint line.

HESSD
10, 325–373, 2013

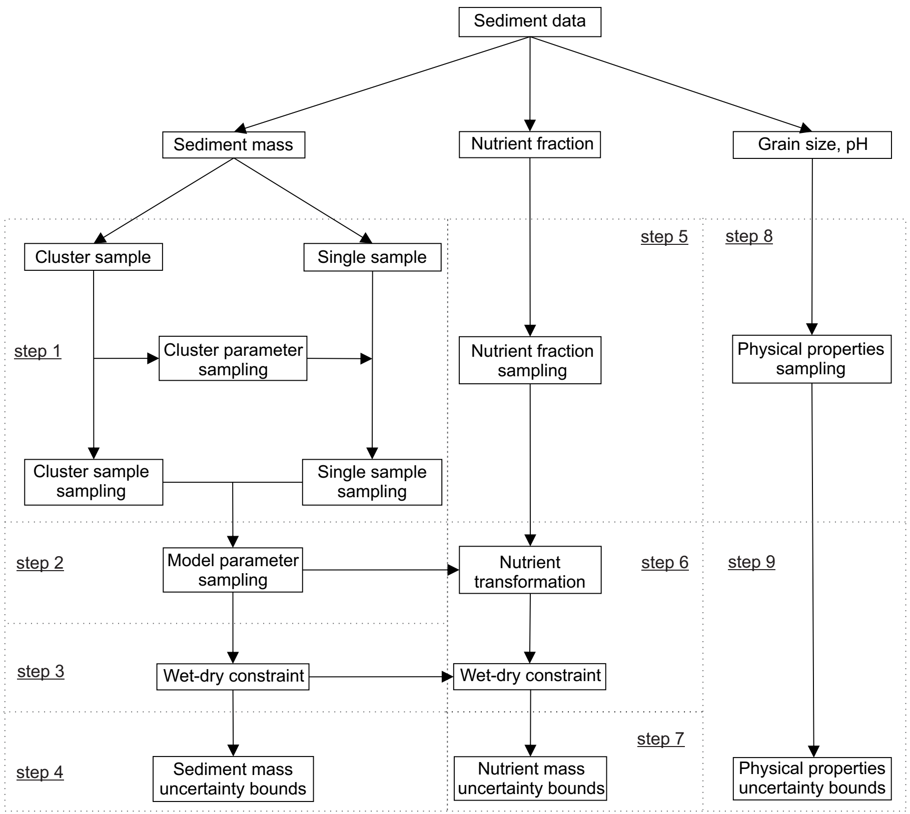

Fig. 7. Uncertainty analysis workflows for sediment mass, nutrient fractions and grain size, pH.

HESSD
10, 325–373, 2013

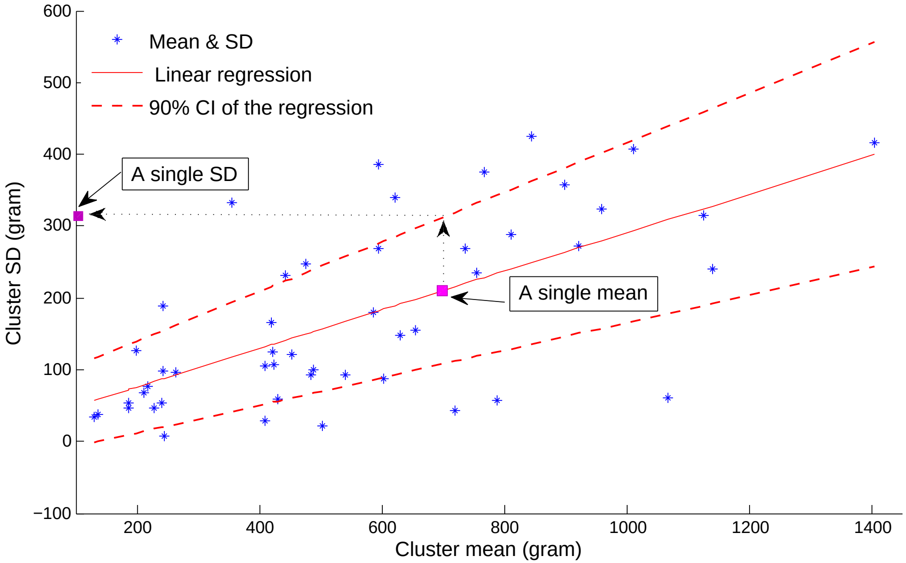

Fig. 8. Linear regression between SD and mean values derived from the multi-trap clusters.

HESSD
10, 325–373, 2013

A case study in the Mekong Delta

N. V. Manh et al.

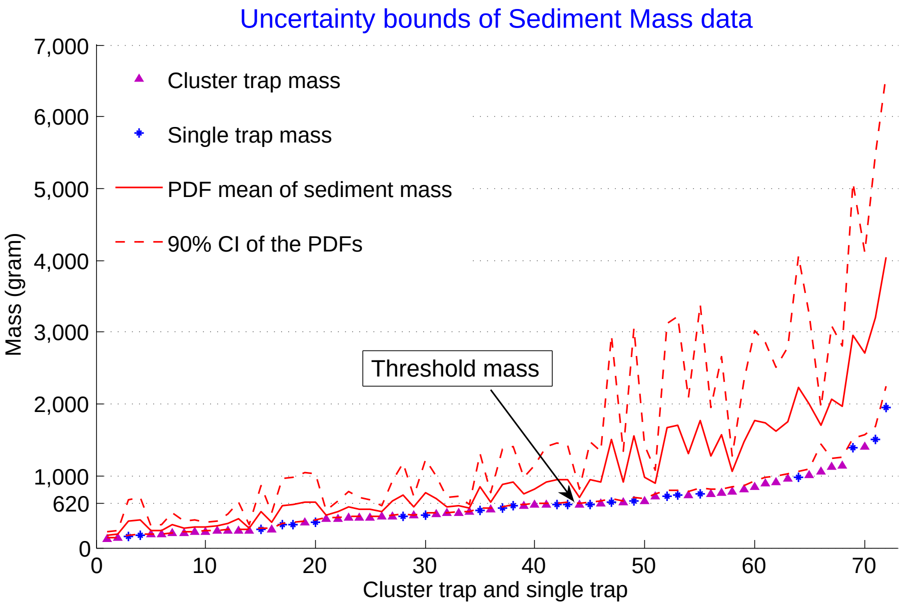

Fig. 9. PDFs mean (red line) and CIs (red dash lines) of sediment mass, and monitored original sediment masses with indication of cluster and single trap samples.

HESSD
10, 325–373, 2013

A case study in the Mekong Delta

N. V. Manh et al.

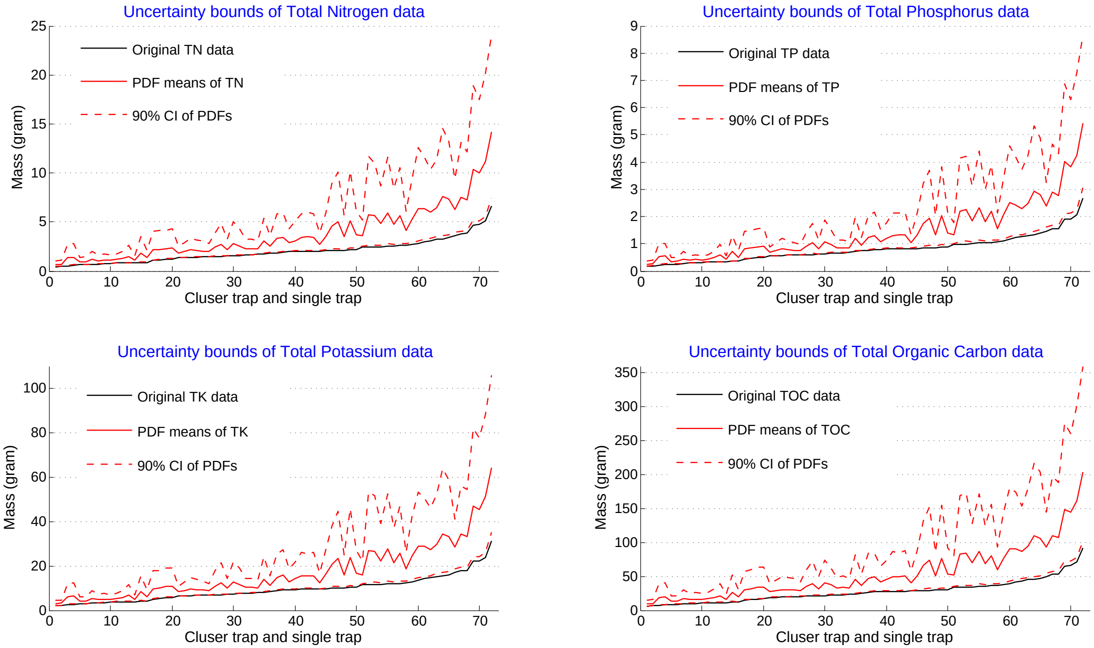

Fig. 10. PDFs mean (red lines) and CIs (red dash lines) of nutrient mass, compare to the original mass (black lines).

HESSD
10, 325–373, 2013

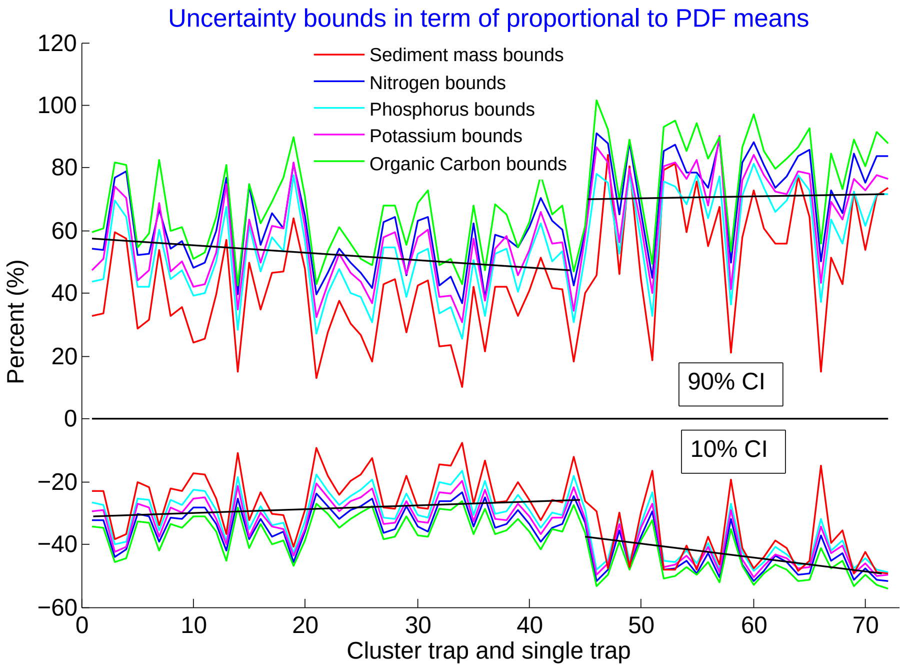

Fig. 11. Relative uncertainty bounds to the means of sediment mass and nutrient mass data.

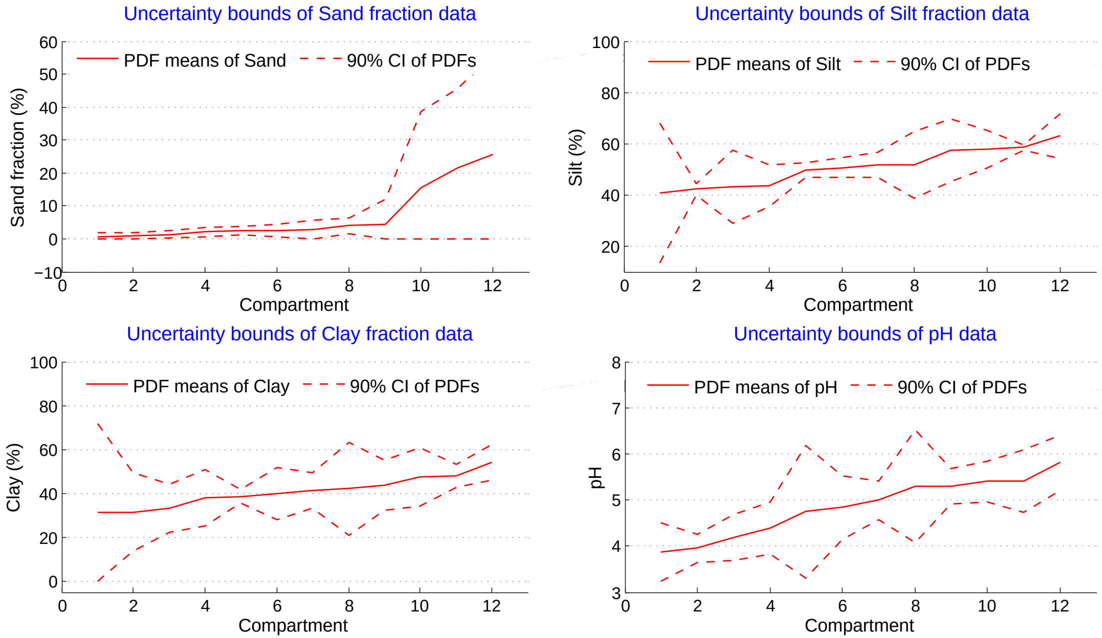

Fig. 12. PDFs mean (red lines) and CIs (red dash lines) of sand fraction, silt fraction, clay fraction and pH.

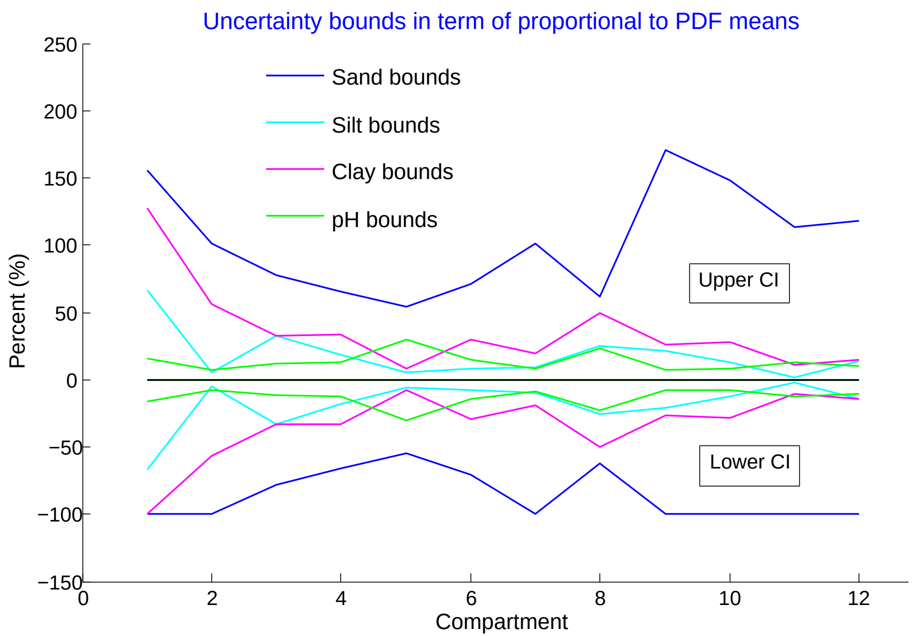

Fig. 13. Relative uncertainty bounds to the means of grain size and pH data.

HESSD
10, 325–373, 2013

A case study in the Mekong Delta

N. V. Manh et al.

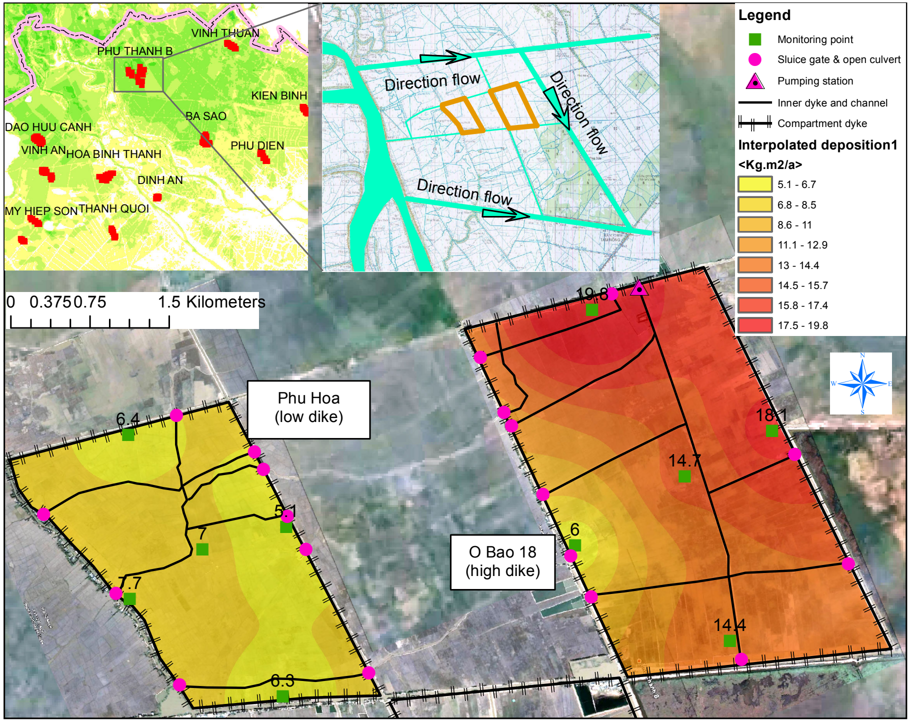

Fig. 14. Spatial distribution of sedimentation in two nearby compartments in Phu Thanh B sites.

HESSD
10, 325–373, 2013

A case study in the Mekong Delta

N. V. Manh et al.

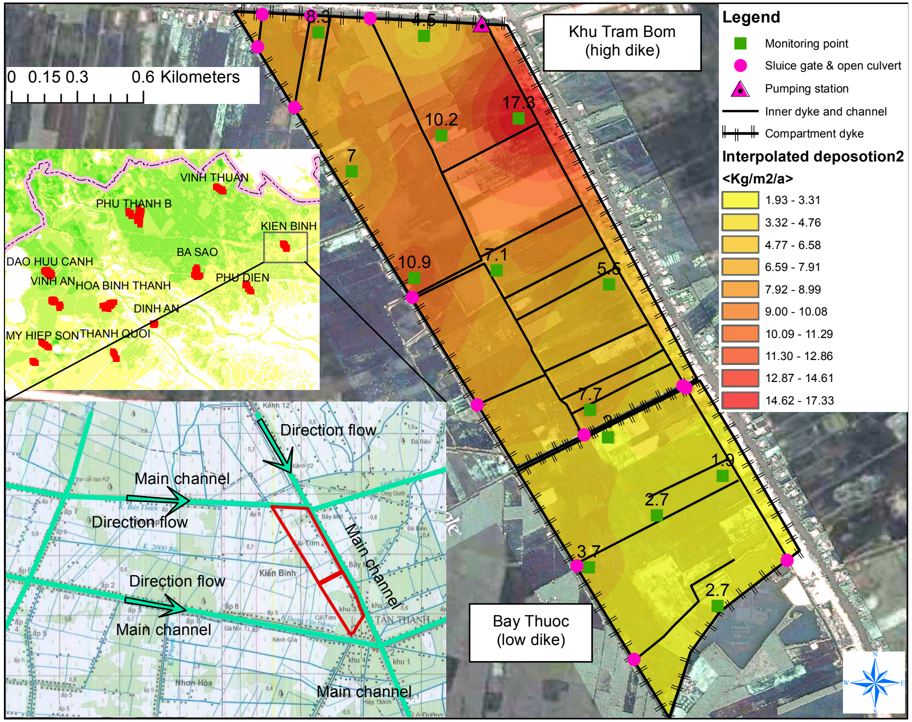

Fig. 15. Spatial distribution of sedimentation in two adjacent compartments in Kien Binh site–Long An.

HESSD
10, 325–373, 2013

A case study in the Mekong Delta

N. V. Manh et al.

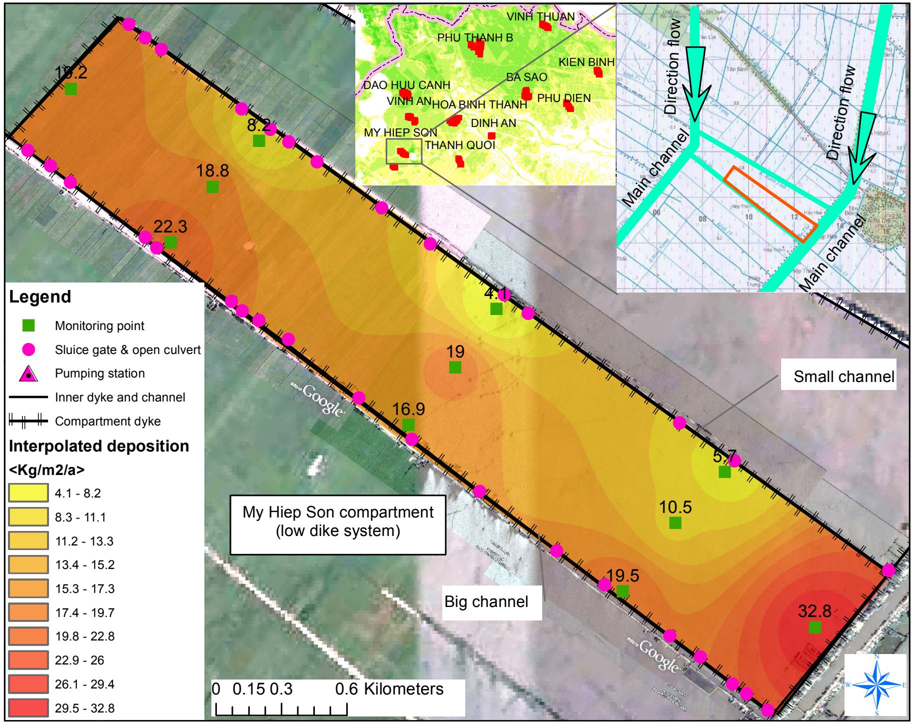

Fig. 16. The typical pattern of high sedimentation variability in low dike compartments in My Hiep Son–Kien Giang.